ECS Transactions, 77 (11) 569-579 (2017) 10.1149/07711.0569ecst ©The Electrochemical Society

Effect of Covalent Chemistry on the Electronic Structure and Properties of the Carbon Allotropes

M. Chen^{a,b}, X. Tian^{a,b}, A. Pekker^{a,c}, W. Li^{a,c}, M. L. Moser^{a,c}, S. Sarkar^{a,c}, F. Wang^{a,d}, D. Stekovic^{a,c}, G. Li^{a,b}, B. Arkook^{a,d}, I. Kalinina^{a,c}, M. E. Itkis^{a-c} and E. Bekyarova^{a-c*}

- ^a Center for Nanoscale Science and Engineering, University of California, Riverside, California 92521, USA
- ^b Department of Chemical and Environmental Engineering, University of California, Riverside, California 92521, USA
- ^c Department of Chemistry, University of California, Riverside, California 92521, USA
- ^d Department of Physics and Astronomy, University of California, Riverside, California 92521, USA

*Corresponding author: elenab@ucr.edu

We discuss advances in the covalent modification of the carbon allotropes, in particular graphene and carbon nanotubes. The main focus is on the organometallic chemistry that affords the possibility to electronically interconnect graphitic surfaces by means of covalent bonding. This mode of functionalization allows the formation of atomic scale interconnects that consist of bishexahapto-metal-bonds between benzenoid ring systems, which increases the dimensionality of the electronic structure of the materials leading to enhanced conductivity. The bis-hexahapto bond formation in single walled carbon nanotubes (SWNTs), graphite nanoplatelets and graphene, can be readily accomplished by metal vapor synthesis (e-beam evaporation), solution and photochemical routes.

Introduction

In the past years, the research directed by Robert C Haddon was focused on the preparation of a new class of carbon materials and modification of their electronic structure and properties through chemistry. The effect of covalent chemistry on the geometric and electronic structures of the carbon allotropes is directly associated with the change of conjugation of the derivatized carbon atoms and this determines two limiting cases. In the conventional addition chemistry, the functionalization leads to the formation of σ-bonds to the graphitic surface and full rehybridization of the carbon atoms from sp² to sp³ (1-4). This destructive rehybridization leads to materials and devices with a decreased conductivity and carrier mobility mobility (5-7). On the other hand it has the potential to bring about interesting magnetic (8, 9) and optoelectronic properties (10). The other limiting case is the constructive rehybridization manifested in the covalent chemisorption of metal atoms on carbon surfaces with formation of an organometallic hexahapto-metal bond that largely preserves the graphitic band structure (11). Importantly, this functionalization of the graphitic surfaces with transition metals allows the formation of atomic scale interconnects and may transform the way contacts are made in future electronics (12-16).

Here we summarize recent advances in the organometallic chemistry of the extended π -conjugated carbon materials, including carbon nanotubes, graphene and graphene nanoplatelets. The prototypical example of these novel structures are the organometallic arene complexes. Reference to the synthesis of small molecule organometallic complexes reveals that the preparation of hexahapto-bis(arene) metal complexes may be accomplished by a number of different routes, but only two have found general application (17): the metal vapor synthesis (MVS) technique (18) and the solution-based Fischer-Hafner process (19).

Below we demonstrate that variants of some of the gas phase MVS and solution-based reactions are capable of realizing the organometallic functionalization of extended, periodic π -electron systems such as SWNTs and graphene (12, 13, 15, 20, 21). The first organometallic chemical reactions were performed utilizing thermal solution-phase reactions with powders of exfoliated graphene and single walled carbon nanotubes, as well as with graphene films supported on Si/SiO₂ and SiC substrates (11, 20). The air sensitivity of the compounds necessitated *in-situ* measurements of their conductivity that were performed with thin films of the carbon allotropes.

Bis-hexahapto bond formation in single-walled carbon nanotube (SWNT) thin film networks with group 6 metals (13)

SWNT networks offer a unique platform to study the effect of the hexahapto-metal bond on the establishment of electrical contact between graphitic surfaces. The electrical resistance of SWNT thin films is known to be dominated by the inter-nanotube junctions (22-24) (Figure 1). Because the percolation in these films is dominated by the internanotube contacts the transport in SWNT films is sensitive to the formation of (η^6 -SWNT)M(η^6 -SWNT) interconnects (M = metal); particularly in the vicinity of the percolation threshold where the conducting pathways become severely limited by the low density of SWNTs. The use of transition metals to interconnect SWNT surfaces represents the first attempt to use covalent bonding to modulate the conductivity of SWNT thin film networks; prior to this work, the covalent functionalization of graphene and SWNTs has led to a decrease in the conductivity and carrier mobility (6, 25).

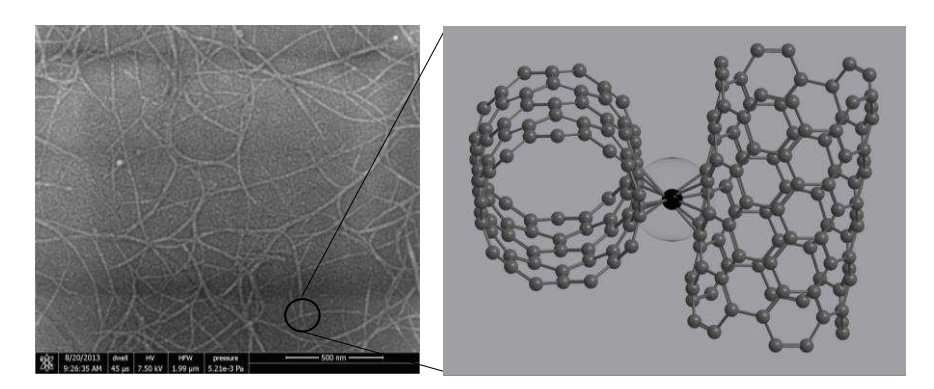


Figure 1. SEM image of single-walled carbon nanotube (SWNT) thin film [left] and schematic of a bis-hexaphato-metal bond interconnecting two SWNTs.

The difference between the hexahapto-metal SWNT interconnects, and the other cases of carbon-metal interaction is demonstrated in Figure 2, which compares the effect of Li

(classic example of a dopant) and gold, a representative transition metal with filled dorbital that cannot form covalent hexahapto-bonds, on the conductivity of SWNT thin film networks. As illustrated in Figure 2 in the initial stage of metal deposition ($t_M < 0.5\,$ ML, ML - monolayer) on semiconducting (SC)-SWNT films, the conductivity enhancement induced by the Cr atoms is significantly stronger than doping by Li. This demonstrates that at very low coverage the ability of Cr to bridge the highly resistive SWNT contacts is always more effective in modulating the electronic properties of SWNT networks, than electron transfer via doping.

Further insight can be gained by comparison of the effect of the metals on the conductivities of SWNT films of different thicknesses: pristine SC-SWNT films below the percolation threshold (t_c : $t_{SWNT} \le 1$ nm) and pristine SC-SWNT films beyond percolation, which have reached the saturation conductivity (Figure 2, $t_{SWNT} \ge 2$ nm).

In the case where the SC-SWNT film is close to the percolation threshold ($t_{SWNT} \le 1$ nm), Cr is always more effective than Li in enhancing the conductivity of the SC-SWNT network (Figure 2a) due to the fact that the film conductivity is severely limited by the number of conducting pathways. At these thicknesses the SC-SWNT film conductivities are extremely dependent on the quality of the inter-nanotube junctions and the conductivity enhancements by the Cr atoms are about a factor of 700 (t = 1 nm) and 700,000 (t = 0.5 nm).

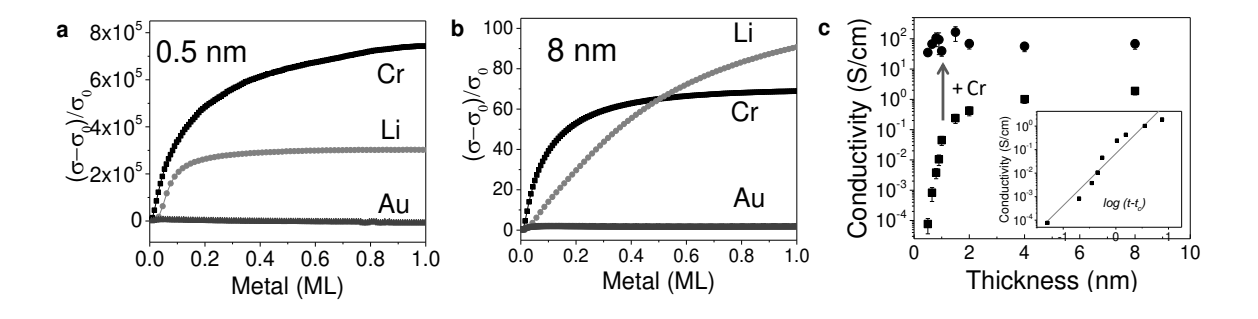


Figure 2. Effect of metal deposition on the electrical conductivity of films of SC-SWNTs of thicknesses: (a) 0.5 nm; (b) 8 nm and (c) Conductivities of SC-SWNT films before (squares) and after (circles) 0.1 ML Cr deposition. Inset of (c) shows a fit of the conductivity data (σ) to the percolation relationship $\sigma \propto (t-t_c)^{\alpha}$, with parameters $t_c \sim 0.45$ nm and $\alpha = 2.2$ (13).

For the SC-SWNT thin films above percolation, Li doping eventually becomes more effective in its ability to enhance the bulk SC-SWNT film conductivity (Figure 2b). Above the percolation threshold, the effect of Cr deposition on the SC-SWNT film conductivities is independent of film thickness which suggests that the formation of (η^6 -SWNT)Cr(η^6 -SWNT) bonds is able to completely remedy the weak links in the SWNT network to the point that percolation effects are no longer apparent in the data (Figure 2c).

The effect of hexahapto bond formation of the conductivities of metallic (MT-) SWNT films is similar to that observed for SC-SWNT films: Cr is always more effective below the saturation conductivity of the pristine films (Figure 3, $t_{SWNT} \le 1$ nm).

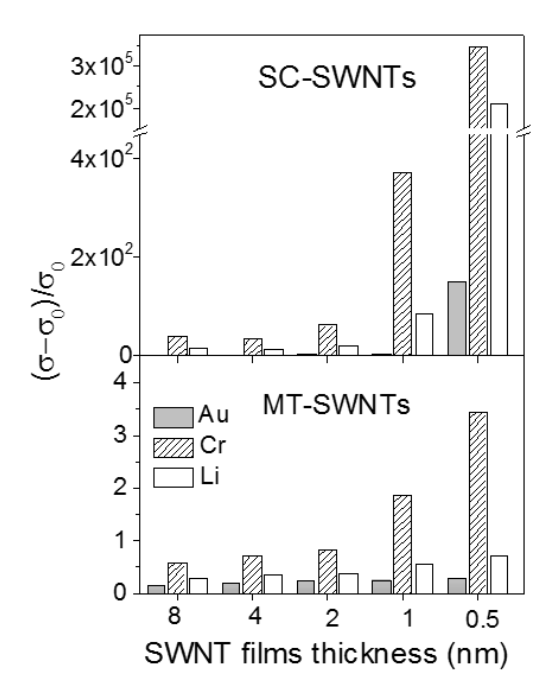


Figure 3. Conductivity enhancements at 0.1 ML of deposited metal for SC- and MT-SWNT films (13).

Effect of Lanthanide Deposition on Thin Films of SWNTs (13, 16)

The evaporation of other transition metals also enhances the conductivities, but chromium gives rise to the highest conductivities of the transition metals studied to date $[M(\eta^6-SWNT)_2]$, where M=Ti, V, Cr, Mn, and Fe] (11, 21, 26), in validation of the 18-electron rule of organometallic chemistry (27). It could be expected that bis-hexahaptometal bonds, which deviate from the 18-electron rule, might be associated with enhanced conductivities due to charge transfer, but in the cases examined to date there is no evidence for this type of bonding (11, 21, 26, 28).

However the deposition of the lanthanide metals on SWNT films resulted in two different trends in the conductivity (σ) enhancement illustrated in Figure 4: (i) enhancement less than Cr and fairly typical of other transition metals in the case of Ln = La, Nd, Gd, Dy, Ho, and (ii) enhancement that exceeded or matched the Cr values for Ln = Sm, Eu, Yb (15, 29). The lanthanide conductivity data was rationalized by reference to a model based on the accessibility of the $4f^m$ $5d^1$ $6s^2$ electronic configuration for the individual lanthanide atoms (30, 31). This model suggests that Sm, Eu and Yb were able to strongly enhance the conductivity of the SWNT films due to the ability of these metals to not only form bis-hexahapto-bonds, but to also transfer charge into the conduction band of the SWNTs due to the symmetry of the frontier molecular orbitals (FMOs) in the lanthanide complexes, and the fact that the partially filled metal 5d-orbitals involved in the interaction lie relatively high in energy in the case of Sm, Eu and Yb (15). Thus, all lanthanides exhibit the initial abrupt increase in SWNT film conductivity at low coverage which is characteristic of Cr, but only Eu, Sm, Yb show the continually increasing conductivity characteristic of Li (Figure 4b). Thus, Eu, Sm, Yb provide the first examples

of mixed covalent–ionic bis-hexahapto bonds (η^6 -SWNT)M(η^6 -SWNT), which was also confirmed with spectroscopic studies (15, 29).

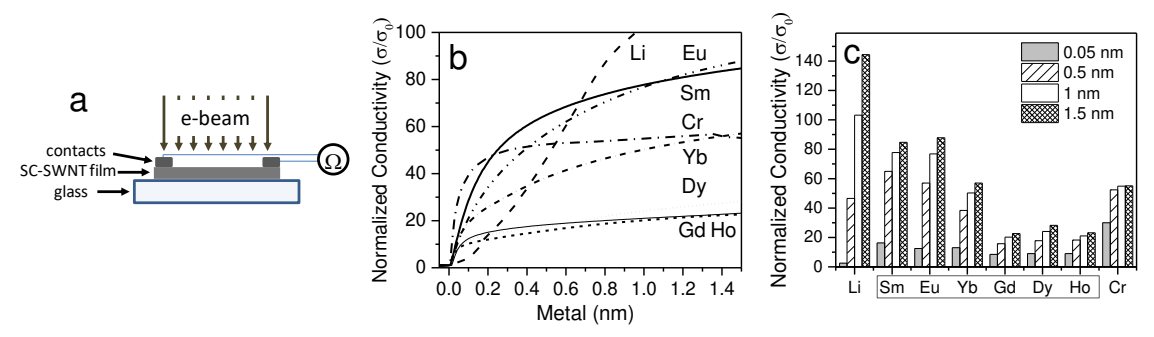


Figure 4. Effect of metal deposition on electrical conductivity of semiconducting (SC-) SWNT films: (a) Schematic illustration of the experimental configuration of the in-situ measurements of the film resistance during e-beam metal evaporation. (b) Change of SC-SWNT film conductivity as a function of deposited metal thickness; the values are normalized to the conductivity of pristine SC-SWNT film, σ_o . (c) Normalized conductivities of SC-SWNT films with deposited metal of thicknesses 0.05, 0.5, 1 and 1.5 nm (29).

Photochemical Generation of Bis-hexahapto Chromium Interconnects Between the Graphene Surfaces of Single-Walled Carbon Nanotubes (14)

It is known that the hexahapto-arene-chromium-tricarbonyls can be prepared by the solution reaction of $Cr(CO)_6$ with the appropriate arene under photochemical conditions (27, 32, 33). The photochemical route was successfully applied for the synthesis of hexahapto graphene-based complexes. The advantage of photochemistry is that it can be accomplished without the need for high vacuum, required in the case of e-beam metal evaporation. The photochemical reactions can be performed in a glove box and are advantageous for preparation of samples for physical characterization.

To explore the photochemical formation of hexahapto bonds between the conjugated surfaces of carbon nanotubes, thin films of three types of SWNTs were prepared: nonseparated (NS-), semiconducting (SC-), and metallic (MT-) SWNTs. The conductivities of the pristine annealed films (thickness 8 nm) at room temperature are as follows: $\sigma \approx 3$ S/cm (SC-SWNT), 350 S/cm (MT-SWNT), 300 S/cm (NS-SWNT). The films, deposited on a glass substrate with gold contacts, were transferred in the glove box and dipped in an acetonitrile solution of the organometallic precursor followed by exposure to light as illustrated in Figure 5a. Figure 5 (b-d) demonstrates that the photochemically induced reactions of $Cr(CO)_6$, $Cr(\eta^6$ -benzene)(CO)₃, and $Cr(\eta^6$ -benzene)₂ with the SWNT films lead to strongly enhanced conductivities and the SC-SWNT films experience the strongest enhancement of the conductivity. The observed conductivity enhancements are as follow: $(\sigma - \sigma_0)/\sigma_0 \approx 100$ (SC-SWNT), 1 (MT-SWNT), 4 (NS-SWNT), where $\sigma =$ SWNT film conductivity after functionalization and σ_0 = pristine SWNT film conductivity. Furthermore, the organometallic reagents exhibit the following order of reactivity $Cr(\eta^6$ -benzene)₂ > $Cr(\eta^6$ -benzene)(CO)₃ > $Cr(CO)_6$ toward the SWNT networks based on the conductivity responses, and all reagents lead to the same final conductivity value.

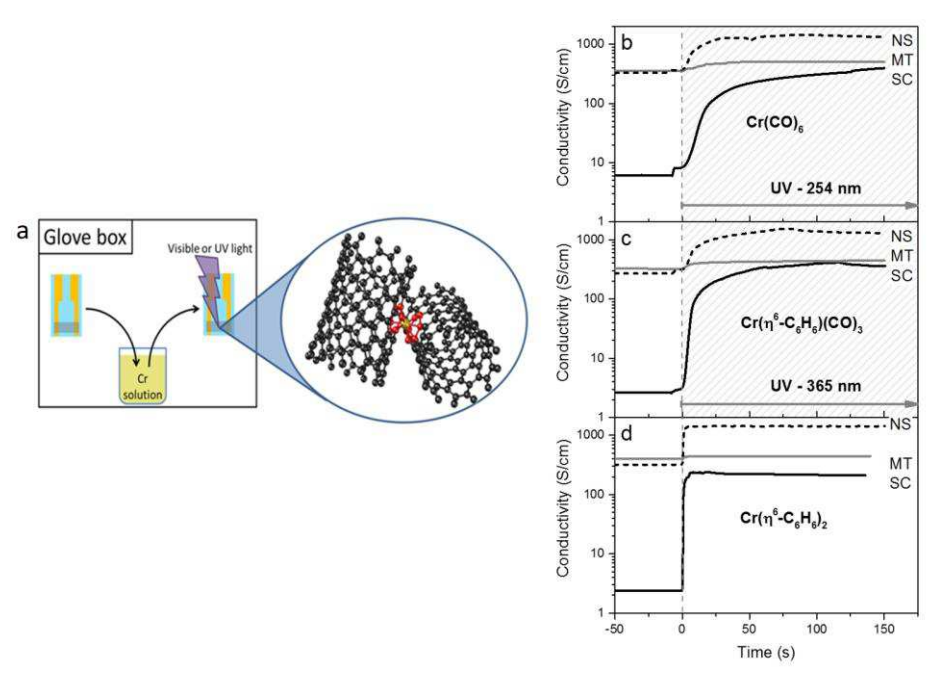


Figure 5. (a) Schematics of the photochemical reaction procedure: After annealing samples were transferred into a glove box and electrically connected for resistance measurement. The samples were dipped into solution of the chromium reagent and irradiated with visible or UV light, which led to the formation of $Cr(\eta^6-SWNT)_2$ complexes at SWNT junctions. (b-d) Evolution of SWNT thin film conductivities on photochemical reaction as a function of SWNT type: semiconducting (SC-), separated metallic (MT-) and nonseparated (NS-) SWNTs. a) photochemical reaction with $Cr(\eta^6$ -benzene)(CO)₃, after irradiation with 365 nm wavelength UVC light. c) reaction with $Cr(\eta^6$ -benzene)₂, after in the presence of room light.

Thus, the photochemical reactions of reagents such as $Cr(CO)_6$, $Cr(\eta^6$ -benzene)(CO)₃, and $Cr(\eta^6$ -benzene)₂ are very effective in forming $Cr(\eta^6$ -SWNT)₂ complexes which act as interconnects between the graphitic surfaces, as evidenced by an abrupt increase in conductivity on irradiation of thin films of these materials in the presence of the appropriate reagents (14).

It was concluded that all three of these reactions lead to the generation of covalent (η^6 -SWNT)Cr(η^6 -SWNT) interconnects which provide conducting pathways in the SWNT films as outlined in the proposed reaction pathways illustrated in Scheme 1.

$$\begin{array}{c} Cr(CO)_{6} & \frac{h\nu}{CH_{3}CN} \underbrace{\frac{(\lambda = 254nm)}{Cr(CH_{3}CN)_{3}(CO)_{3}}} \underbrace{\frac{h\nu}{CH_{3}CN}} \underbrace{\frac{(\lambda = 254nm)}{Cr(\eta^{6}\text{-SWNT})(CO)_{3}}} \underbrace{\frac{h\nu}{CH_{3}CN}} \underbrace{\frac{(\lambda = 254nm)}{Cr(\eta^{6}\text{-SWNT})(CH_{3}CN)_{3}}} \underbrace{\frac{h\nu}{CH_{3}CN}} \underbrace{\frac{(\lambda = 254nm)}{Cr(\eta^{6}\text{-SWNT})_{2}}} \underbrace{\frac{(\lambda = 254nm)}{Cr(\eta^{6}\text{-SWNT})_{2}}} \underbrace{\frac{(\lambda = 365nm)}{CH_{3}CN}} \underbrace{\frac{(\lambda = 365nm)}{Cr(\eta^{6}\text{-SWNT})(CO)_{3}}} \underbrace{\frac{(\lambda = 365nm)}{Cr(\eta^{6}\text{-SWNT})(CO)_{3}} \underbrace{\frac{(\lambda = 365nm)}{Cr(\eta^{6}\text{-SWNT})(CO)_{3}}} \underbrace{\frac{(\lambda = 365nm)}{Cr(\eta^{6}\text{-SWNT})(CO)_{3}} \underbrace{\frac{(\lambda = 365nm)}{Cr(\eta^{6}\text{-SWNT})(CO)_{3}} \underbrace{\frac{(\lambda = 365nm)}{Cr(\eta^{6}\text{-SWNT})(CO)_{3}}} \underbrace{\frac{(\lambda = 365nm)}{Cr(\eta^{6}\text{-SWNT})(CO)_{3}} \underbrace{\frac{(\lambda = 365nm)}{Cr(\eta^{6}\text{-SWNT})(CO)_{3}}} \underbrace{\frac{(\lambda = 365nm)}{Cr(\eta^{6}\text{-SWNT})(CO)_{3}} \underbrace{\frac{(\lambda = 365nm)}{Cr(\eta^{6}\text{-SWNT})(CO)_{3}} \underbrace{\frac{(\lambda = 365nm)}{Cr(\eta^{6}\text{-SWNT})(CO)_{3}}} \underbrace{\frac{(\lambda = 365nm)}{Cr(\eta^{6}\text{-SWNT})(CO)_{3}} \underbrace{\frac{(\lambda = 365nm)}{Cr(\eta^{6}\text{-SWNT})(CO)_$$

Scheme 1. Schematic of the mechanism for the photochemical reactions of single-walled carbon nanotubes (SWNTs) with $Cr(CO)_6$, $Cr(\eta^6-C_6H_6)(CO)_3$ and $Cr(\eta^6-C_6H_6)_2$ (14).

Hexahapto - Metal - GNP Complexes

Graphene nanoplatelets (GNPs) are a very attractive candidate for large scale applications of graphene-based materials (34-37). In the first attempt to prepare bulk graphene materials with interconnected sheets, the graphene-metal complexes, synthesized by solution phase chemistry, were heated under vacuum and external pressure to remove the carbonyls and cross-link the graphene layers with the metal atoms (38). This procedure was not successful in enhancing the conductivity of exfoliated GNPs (38), perhaps due to the large particle sizes of the GNPs and the exposure of the samples to the atmosphere during preparation (36, 38).

With the use of a new form of GNPs prepared by the PPG Industries (PPG GNPs) it was possible to further explore the organometallic chemistry of GNPs. The size of these GNPs is much smaller than that of the conventional exfoliated GNPs prepared from natural graphite (38). The PPG material possesses a crinkled morphology which facilitates the interconnection of the graphene surfaces of different GNPs and allows the formation of bis-hexahapto bonds between adjoining graphene surfaces within distorted individual GNPs, thereby allowing the formation of a novel 3D-connected material, as illustrated in Figure 6.

For these experiments films of PPG with a thickness $t \approx 100$ nm were prepared by spraying dispersions of the material in THF. Three groups of metals:(a) Au, (b) Li, and (d) Cr, Mo, and W, were deposited on the GNP films by e-beam evaporation.

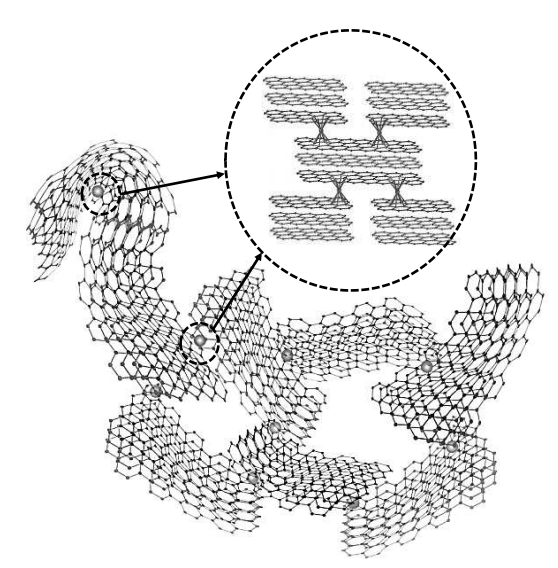


Figure 6. Schematic of the formation of metal complexes with the surface of PPG GNPs.

The change of the film conductivity is illustrated in Figure 7a. Gold shows a very weak effect, as expected for physisorption (11, 39-41), lithium shows clear evidence of charge transfer (ionic chemisorptions) with donation of electrons into the conduction band of the PPG GNPs and a strongly enhanced conductivity.

To understand the interaction between the graphene surface and bare transition metal chromium (Cr) atoms experiments with a single layer CVD graphene (SLG) were also conducted. Figure 7b shows that after evaporating 0.6 nm Cr on the top surface of SLG, the conductivity decreased from $\sigma = 1.15 \times 10^4$ S/cm to $\sigma = 4 \times 10^3$ S/cm, which was assigned to electron scattering from the Cr atoms. STM experiments indicate that Cr atoms are mobile on graphene surfaces and are attracted to defects and contaminants (40), and the formation of clusters has been observed on graphitic surfaces (40) and carbon nanotubes (16, 28, 42).

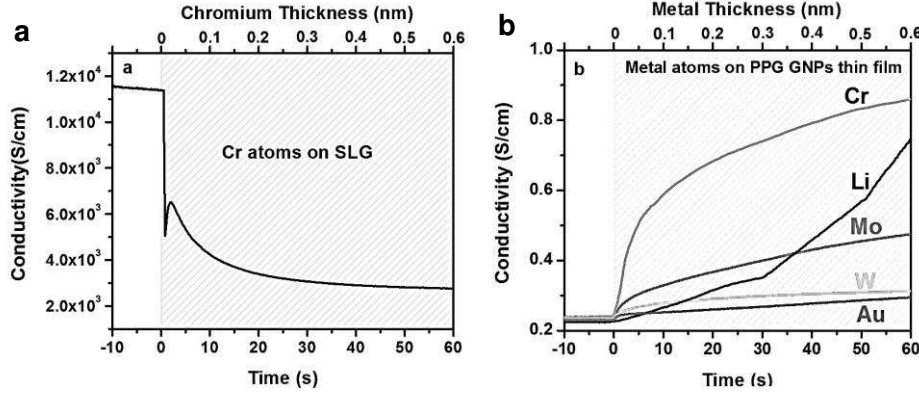


Figure 7. Response of the conductivities of graphene films to metal atom deposition by e-beam as a function of metal thickness: (a) Single layer graphene - SLG, (b) PPG GNP films (thickness 100 nm) (43).

When Cr atoms (0.6 nm) were evaporated onto the PPG GNP thin films, the conductivity of the films increased from $\sigma = 0.22$ S/cm to 0.82 S/cm, which contrasts with the result obtained on evaporation of Cr on SLG sheets (Figure 7a). It appears that the Cr atoms are able to bridge some of the nanoplatelets and to spontaneously form

covalent bis(η^6 -GNP)Cr bonds that enhance the film conductivity. The conductivity was enhanced by a factor of about three to four which is very similar to the values found on deposition of Cr on metallic (MT)-SWNT films (13)]. The evaporation of other group 6 metals such as molybdenum (Mo) and tungsten (W), onto the PPG GNP films also enhances the conductivities, but the increases are much more modest.

Figure 8 illustrates the effect of the photochemical reaction of the PPG GNP films with organometallic reagents on the conductivity of GNP films. The lower traces of Figure 8a show the effect of the reagent alone and of a blank UV irradiation experiment. It is clear that the simultaneous application of the reagent together with UV light (UVC, 254 nm) is necessary to initiate the reaction. Irradiation with UVC light in the presence of $Cr(CO)_6$ leads to an increase in the conductivity of the PPG GNP thin film from $\sigma = 0.22$ S/cm to 0.9 S/cm, which is consistent with the MVS results (Figure 7b).

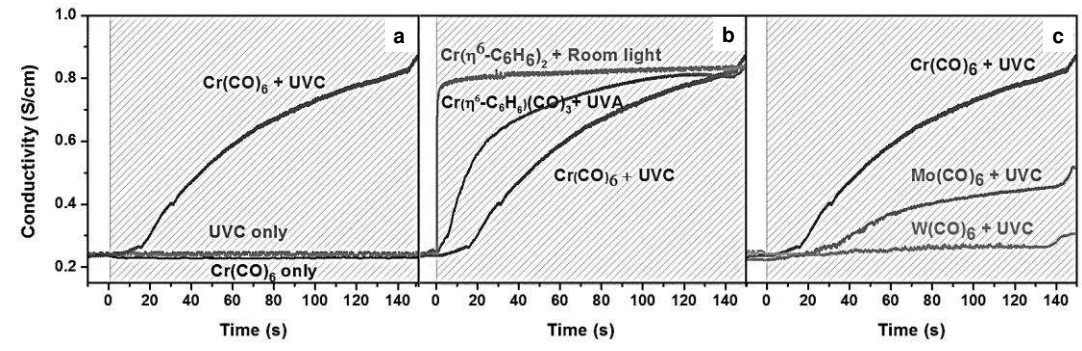


Figure 8. Evolution of PPG GNP thin film conductivities on photochemical reaction with organometallic reagents (thickness, $t \approx 100$ nm) (43).

These results are in accord with the conductivity enhancement of SWNT films subjected to photochemical reaction with organometallic reagents, suggesting that the same mechanism operates in the case of GNP and SWNT films (14). Figure 8b compares the reactivity of the chromium reagents with the GNP films, which follows the sequence $Cr(CO)_6 < Cr(\eta^6\text{-benzene})(CO)_3 < Cr(\eta^6\text{-benzene})_2$. Nevertheless the final conductivities are very close and it is apparent that the same final material composition is achieved irrespective of the organometallic reagent. The $Mo(CO)_6$ and $W(CO)_6$ reagents also react with the GNP films under UVC light, but the final conductivities are significantly lower than in the case of the Cr compounds (Figure 8c). The conductivities of the new 3D cross-linked GNP materials, synthesized by the photochemical route, are consistent with those obtained by the MVS method (Figure 7), which further supports the fact the proposed mechanisms in Scheme 1 are also operating in the case of GNPs.

Conclusions

The organometallic bis-hexahapto bond offers a unique route to electronically interconnects the conjugated surfaces of the periodic π -electron systems present in carbon nanotubes and graphene by means of covalent bonding. The preparation of the transition metal-carbon nanomaterials can be accomplished using three approaches: vapor-phase chemistry, solution phase chemistry, and photochemistry. The hexahapto organometallic bond offers the only possibility to bridge the π -systems of the carbon allotropes in a manner which preserves the delocalization within the subunits and also offers a seamless

electronic interconnection between the conjugated fragments. Another key outcome is the demonstration of the first example of mixed covalent—ionic bis-hexahapto bond in compounds formed on interaction of the lanthanide metals M = Sm, Eu with carbon nanotube films.

The organometallic graphene chemistry may lead to the development of a class of novel transition metal-graphene materials that exhibit unique electronic properties, and it may lay the foundation for interconnects between graphitic surfaces at the atomic level. The studies provide a foundation for the synthesis of organometallic graphene materials, expand the fundamental understanding of the effect of metal coordination on the electronic structure of graphene and enrich the knowledge of metal-graphene interactions.

Acknowledgements

This work is dedicated to Robert C Haddon. The study of the organometallic reactions with carbon nanomaterials was supported by NSF under contract DMR-1305724.

References

- 1. S. Niyogi, M. A. Hamon, H. Hu, B. Zhao, P. Bhowmik, R. Sen, M. E. Itkis and R. C. Haddon, *Acc. Chem. Res.* **35**, 1105 (2002).
- 2. B. Zhao, H. Hu, E. Bekyarova, M. E. Itkis, S. Niyogi and R. C. Haddon, *Dekker Encyclopedia of Nanoscience and Nanotechnology*, 493 (2004).
- 3. E. Bekyarova, M. E. Itkis, P. Ramesh and R. C. Haddon, *Phys. Stat. Sol. RRL* 3, 184 (2009).
- 4. S. Niyogi, E. Bekyarova, J. Hong, S. Khizroev, C. Berger, W. A. de Heer and R. C. Haddon, *J. Phys. Chem. Lett.* **2**, 2487 (2011).
- 5. E. Bekyarova, M. E. Itkis, P. Ramesh, C. Berger, M. Sprinkle, W. A. de Heer and R. C. Haddon, *J. Am. Chem. Soc.* **131**, 1336 (2009).
- 6. H. Zhang, E. Bekyarova, J.-W. Huang, Z. Zhao, W. Bao, F. Wang, R. C. Haddon and C. N. Lau, *Nano Lett.* **11**, 4047 (2011).
- 7. S. Sarkar, E. Bekyarova and R. C. Haddon, *Mater. Today* **15**, 276 (2012).
- 8. J. Hong, S. Niyogi, E. Bekyarova, M. E. Itkis, R. Palanisamy, N. Amos, D. Litvinov, C. Berger, W. A. de Heer, S. Khizroev and R. C. Haddon, *Small* **7**, 1175 (2011).
- 9. J. Hong, E. Bekyarova, P. Liang, W. A. de Heer, R. C. Haddon and S. Khizroev, *Sci. Rep.* **2**, 624 (2012).
- 10. P. Ramesh, M. E. Itkis, E. Bekyarova, F. Wang, S. Niyogi, X. Chi, C. Berger, W. A. de Heer and R. C. Haddon, *J. Am. Chem. Soc.* **132**, 14429–14436 (2010).
- 11. F. Wang, M. E. Itkis, E. Bekyarova, X. Tian, S. Sarkar, A. Pekker, I. Kalinina, M. Moser and R. C. Haddon, *Appl. Phys. Lett.* **100**, 223111 (2012).
- 12. S. Sarkar, M. L. Moser, X. Tian, X. J. Zhang, Y. F. Al-Hadeethi and R. C. Haddon, *Chem. Mater.* **26**, 184 (2014).
- 13. X. Tian, M. L. Moser, A. Pekker, S. Sarkar, J. Ramirez, E. Bekyarova, M. E. Itkis and R. C. Haddon, *Nano Lett.* **14**, 3930 (2014).
- 14. A. Pekker, M. Chen, E. Bekyarova and R. C. Haddon, *Mater. Horiz.* 2, 81 (2015).
- 15. M. L. Moser, X. Tian, A. Pekker, S. Sarkar, E. Bekyarova, M. E. Itkis and R. C. Haddon, *Dalton Trans.* **43**, 7379 (2014).

- 16. I. Kalinina, Y. F. Al-Hadeethi, E. Bekyarova, C. Zhao, Q. Wang, X. Zhang, A. Al-Zahrani, F. Al-Agel, F. Al-Marzouki and R. C. Haddon, *Mater. Lett.* **142**, 312 (2015).
- 17. G. Pampaloni, Coord. Chem. Rev. 254, 402 (2010).
- 18. P. L. Timms, Chem. Commun., 1033 (1969).
- 19. E. O. Fischer and W. Hafner, Z. Naturf. 10b, 665 (1955).
- 20. S. Sarkar, S. Niyogi, E. Bekyarova and R. C. Haddon, *Chem. Sci.* **2**, 1326 (2011).
- 21. E. Bekyarova, S. Sarkar, F. Wang, M. E. Itkis, I. Kalinina, X. Tian and R. C. Haddon, *Acc. Chem. Res.* **46**, 65 (2013).
- 22. L. Hu, D. S. Hecht and G. Gruner, Nano Lett. 4, 2513 (2004).
- 23. E. Bekyarova, M. E. Itkis, N. Cabrera, B. Zhao, A. Yu, J. Gao and R. C. Haddon, *J. Am. Chem. Soc.* **127**, 5990 (2005).
- 24. M. E. Itkis, A. Pekker, X. Tian, E. Bekyarova and R. C. Haddon, *Acc. Chem. Res.* **48**, 2270 (2015).
- 25. S. Sarkar, H. Zhang, J.-W. Huang, F. Wang, E. Bekyarova, C. N. Lau and R. C. Haddon, *Adv. Mater.* **25**, 1131 (2013).
- 26. F. Wang, M. E. Itkis, E. Bekyarova, S. Sarkar, X. Tian and R. C. Haddon, *J. Phys. Org. Chem.* **25** (7), 607 (2012).
- 27. C. Elschenbroich, Organometallics. Third ed.; Wiley-VCH: Weinheim, 2006.
- 28. I. Kalinina, E. Bekyarova, S. Sarkar, F. Wang, M. E. Itkis, X. Tian, S. Niyogi, N. Jha and R. C. Haddon, *Macromol. Chem. Phys.* **213**, 1001 (2012).
- 29. M. L. Moser, A. Pekker, X. Tian, E. Bekyarova, M. E. Itkis and R. C. Haddon, *ACS Appl. Mat. Interfaces* **7**, 28013 (2015).
- 30.D. M. Anderson, F. G. N. Cloke, P. A. Cox, N. Edelstein, J. C. Green, Tanya Pang, A. A. Sameh and G. Shalimoff, *J. Chem. Soc.*, *Chem. Commun.*, 53 (1989).
- 31. F. G. N. Cloke, Chem. Soc. Rev., 17 (1993).
- 32. G. B. M. Kostermans, M. Bobeldijk, W. H. d. W. Kwakman and F. Bickelhaupt, *J. Organomet. Chem.* **363**, 291 (1989).
- 33. E. P. Kundig, Topics Organomet. Chem. 7, 3 (2004).
- 34. S. Biswas and L. T. Drzal, *Nano Lett.* **9**, 167 (2009).
- 35. M. Lotya, Y. Hernandez, P. J. King, R. J. Smith, V. Nicolosi, L. S. Karlsson, F. M. Blighe, S. De, Z. M. Wang, I. T. McGovern, G. S. Duesberg and J. N. Coleman, *J. Am. Chem. Soc.* **131**, 3611 (2009).
- 36. X. Sun, P. Ramesh, M. E. Itkis, E. Bekyarova and R. C. Haddon, *J. Phys.: Condens. Matter* **22**, 334216 (2010).
- 37. S. Biswas, H. Fukushima and L. T. Drzal, *Compos. Part A Appl. Sci. Manuf.* **42**, 371 (2011).
- 38. X. Tian, S. Sarkar, M. L. Moser, F. Wang, A. Pekker, E. Bekyarova, M. E. Itkis and R. C. Haddon, *Mater. Lett.* **80**, 171 (2012).
- 39. K. T. Chan, J. B. Neaton and M. L. Cohen, *Phys. Rev. B* 77, 235430 (2008).
- 40. R. Zan, U. Bangert, Q. Ramasse and K. S. Novoselov, Nano. Lett. 11, 1087 (2011).
- 41.X. Liu, C.-Z. Wang, M. Hupalo, H.-Q. Lin, K.-M. Ho and M. C. Tringides, *Crystals* **3**, 79 (2013).
- 42. I. Kalinina, E. Bekyarova, Q. Wang, Y. F. Al-Hadeethi, X. J. Zhang, F. Al-Agel, F. Al-Marzouki, S. Yaghmour and R. C. Haddon, *Fuller. Nanotub. Carb. N.* **22**, 47 (2014).
- 43. M. Chen, X. Tian, W. Li, E. Bekyarova, G. Li, M. Moser and R. C. Haddon, *Chem. Mater.* **28**, 2260 (2016).